Non-Linear Shipboard Shock Analysis of the TOMAHAWK Missile Shock Isolation System

Joel Leifer
Michael Gross

The identification, quantification, computer modeling and verification of the TOMAHAWK non-linear liquid spring shock isolation system in the surface ship Vertical Launch System (VLS) are discussed. The isolation system hardware and mode of operation is detailed in an effort to understand the non-linearities. These non-linearities are then quantified and modeled using the MSC/NASTRAN finite element code. The model was verified using experimental data from the Naval Ordnance Systems Center (NOSC) MIL-S-901 medium-weight shock tests of Aug. 1986. The model was then used to predict the TOMAHAWK response to the CG-53 USS MOBILE BAY shock trials of May-June 1987. Results indicate that the model is an accurate mathematical representation of the physical system either functioning as designed or in an impaired condition due to spring failure.

INTRODUCTION

This paper presents the analysis and predicted response of the TOMAHAWK CG53/VLS shock isolation system during shipboard shock. The analysis was complicated by the need to identify and quantify several non-linearities. The heart of the shock isolation system analyzed is an assembly of liquid springs. The function of each assembly was non-linear due to geometric clearance (gapping) and loading as a non-linear function of displacement and velocity. These springs work in conjunction with the sixteen friction pads that are attached to the MK-14 canister and grip the AUR.

The VLS is a modular construction consisting of eight cells. Seven of the cells contain eight encanistered missiles each. The eighth cell contains five encanistered missiles and a strikedown crane. The missiles are TOMAHAWK cruise, Standard Missile Two and Vertical Launch ASROC. The isolation system study applies only to the TOMAHAWK missile in the MK 14 Canister.

LIQUID SPRING HARDWARE

The liquid spring system considered in this paper is designed to isolate the TOMAHAWK missile in the surface ship Vertical Launch System from shipboard shock caused by nearby underwater explosions. Each missile/All-Up Round (AUR) configuration has its own integral shock isolation system containing four liquid spring assemblies. Each assembly has a primary and secondary liquid spring working in opposite directions. The secondary spring has the ability to isolate itself from the system during the initial pulse by lifting off of its bearing surface (gapping). Each spring has a resetting spring force that is a quadratic function of the relative displacement and a damping force (that varies depending on whether the spring is in compression or extension). This damping force is a function of the velocity to a power of .7 as specified on the procurement drawings.

MODE OF OPERATION

The liquid spring assembly experiences four distinct conditions or modes of operation as it performs its job. These conditions are :

1) Primary in compression and compressing, secondary gapped - condition 1
2) Primary in compression but extending, secondary gapped - condition 2
3) Primary in compression but extending, secondary in compression and compressing - condition 3
4) Primary in compression and compressing, secondary in compression but extending - condition 4

A plot of a typical spring assembly response is shown in Figure 1 with the occurrence of each condition labeled. The four conditions are discussed in more detail in the following paragraphs.

The secondary spring is preloaded by pressurizing the cylinder. This forces the piston to its full one inch displacement. The two springs are then loaded into the strut and the primary spring is preloaded by torquing the bolt that bears on the secondary spring (see Figure 2) to a one inch displacement. The two springs are in series, but, since the secondary is so much stiffer than the primary, it acts as a semi-rigid bar and transfers most of the load (and hence the deflection) into the primary spring. The AUR is then installed, reducing the preload in the primary spring by an amount equal to its weight of 3600 lbs. This is the steady state condition.

Condition 1 (see Figure 3) commences when the system is subjected to a transient excitation in the vertical or X direction. The

FIGURE 1 TYPICAL SPRING ASSEMBLY RESPONSE

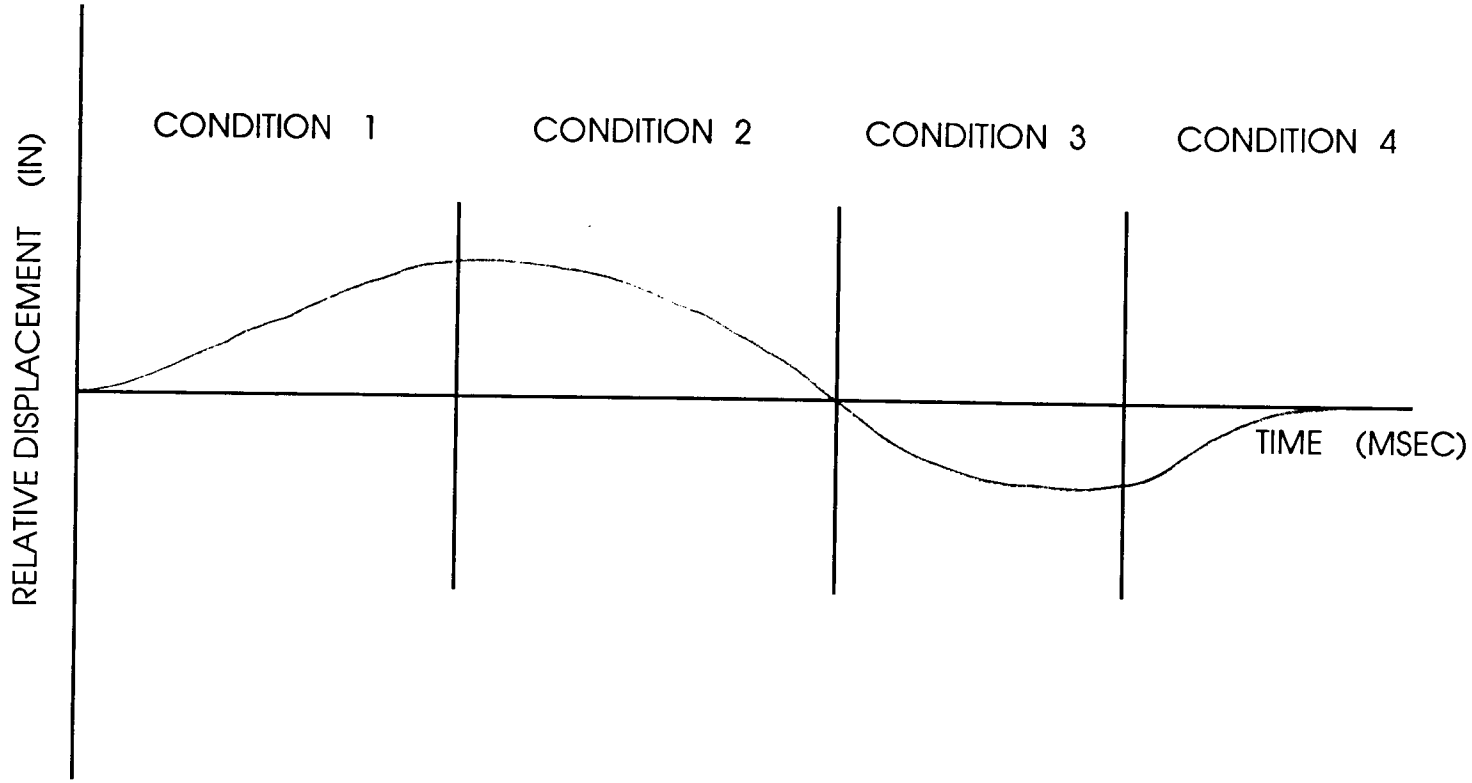

FIGURE 2 LIQUID SPRING ASSEMBLY GEOMETRY

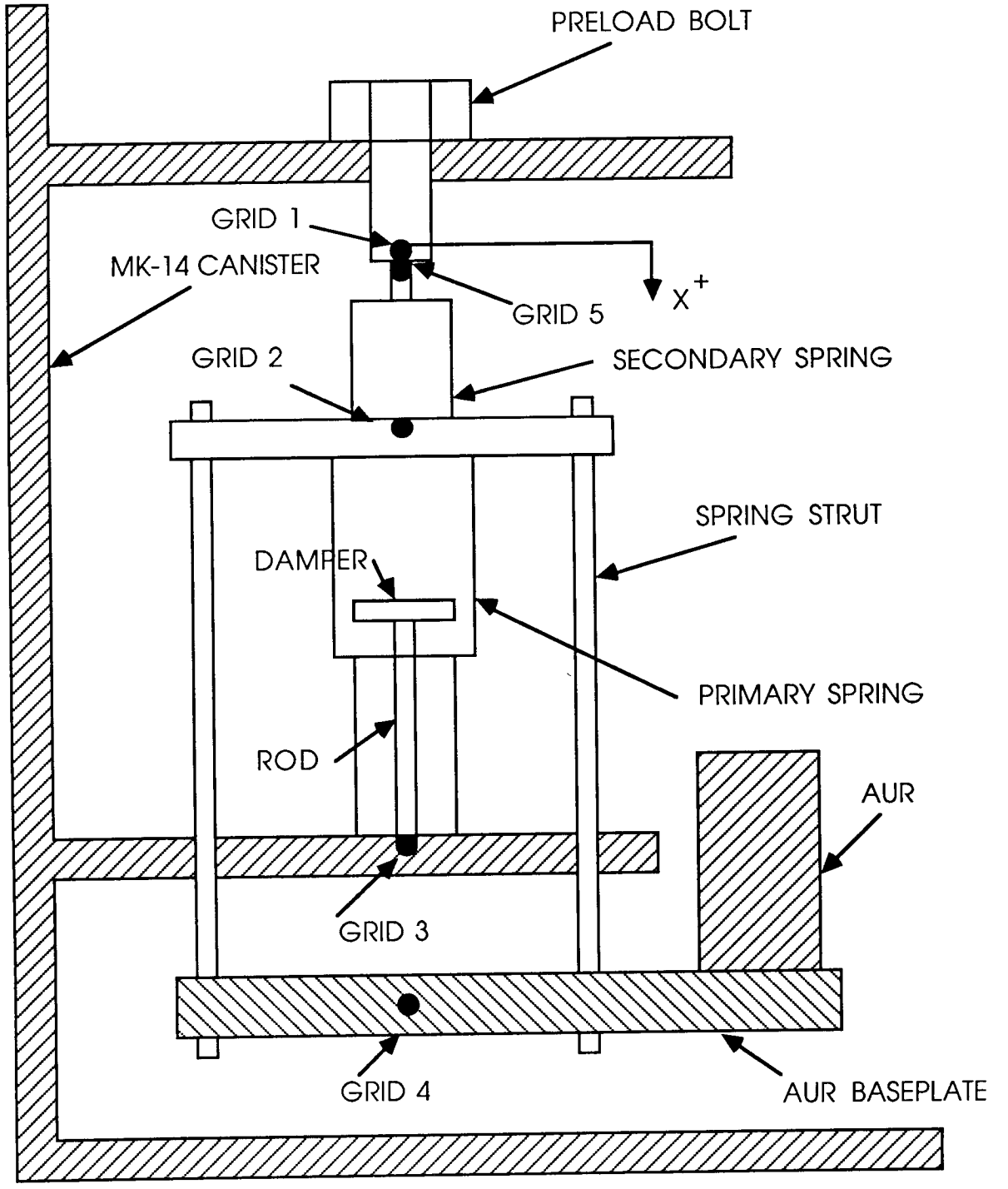

FIGURE 3 PRIMARY IN COMPRESSION AND COMPRESSING, SECONDARY GAPPED

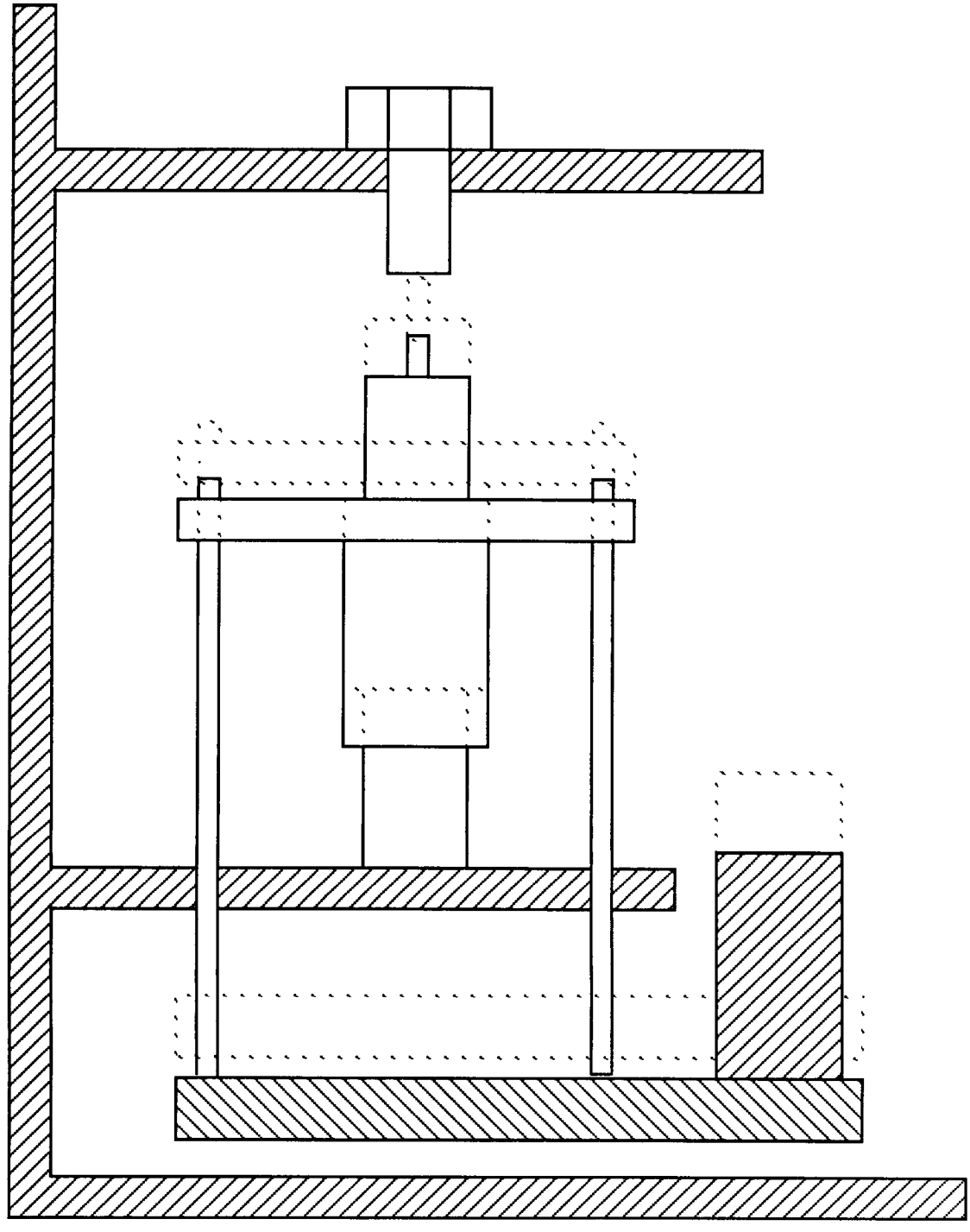

resulting load path is from the MK-14 Canister, thorough the liquid spring assemblies and into the AUR. Initially, the MK-14 Canister will move in the X- direction (see Figure 2 for coordinate system definition), compressing the primary spring. The secondary spring will gap when the compression force generated in the primary spring overcomes the remaining primary preload. This remaining preload is the difference between the initial preload caused by the one inch compression and the weight of the AUR.

When the acceleration in the X+ direction is of sufficient force to overcome the momentum in the opposite direction the relative displacement will have peaked and will begin to decline. This signals the start of condition 2 (see Figure 4). At this time the primary spring (which has been compressed) will start to extend. The spring force stored in the primary spring will add to the acceleration generated force. The secondary spring will remain gapped until the primary spring releases its stored spring force by extending to its original length. The gap will close at the same condition it opened at, ie, when the force generated in the primary spring by the applied load is equal to the remaining preload.

The momentum continues in the same direction as in the previous condition causing the primary to pass to its equilibrium position and try to extend. At its equilibrium position, however, the secondary will have closed its gap and will attempt to bear the load. At this point (the start of condition 3, Figure 5) any compression of the secondary is accompanied by an equal extension of the primary. The total load on the secondary is the sum of the applied force and the stored spring force in the primary. For this analysis, any impact forces generated by the gap closing are ignored.

At the start of condition 4 (Figure 6) the momentum has shifted to the X- direction, and the extension in the primary and compression in the secondary have peaked. The secondary will start to extend, releasing its stored spring energy in the form of a force which adds to the acceleration developed force. The sum of these forces is absorbed by the compressing of the primary spring.

FINITE ELEMENT MODEL

The MSC/NASTRAN [1] finite element computer code was used to analyze the missile response. MSC/NASTRAN employs the finite element method to assemble a mathematical model based on user supplied parameters describing the structure and loading. This model is solved using a numerical integration technique that steps through time. The code requires the user to define physical hardware locations (grid points) and connections (elements) that will result in a mathematical model representing the system under analysis. The associated geometry, element selection, and loading are discussed in the following paragraphs.

The grid points are located using the geometry shown in Figure 2. Grid point one is located on the end of the preload bolt above the secondary spring. Grid point five is at the end of the secondary

FIGURE 4 PRIMARY IN COMPRESSION BUT EXTENDING, SECONDARY GAPPED

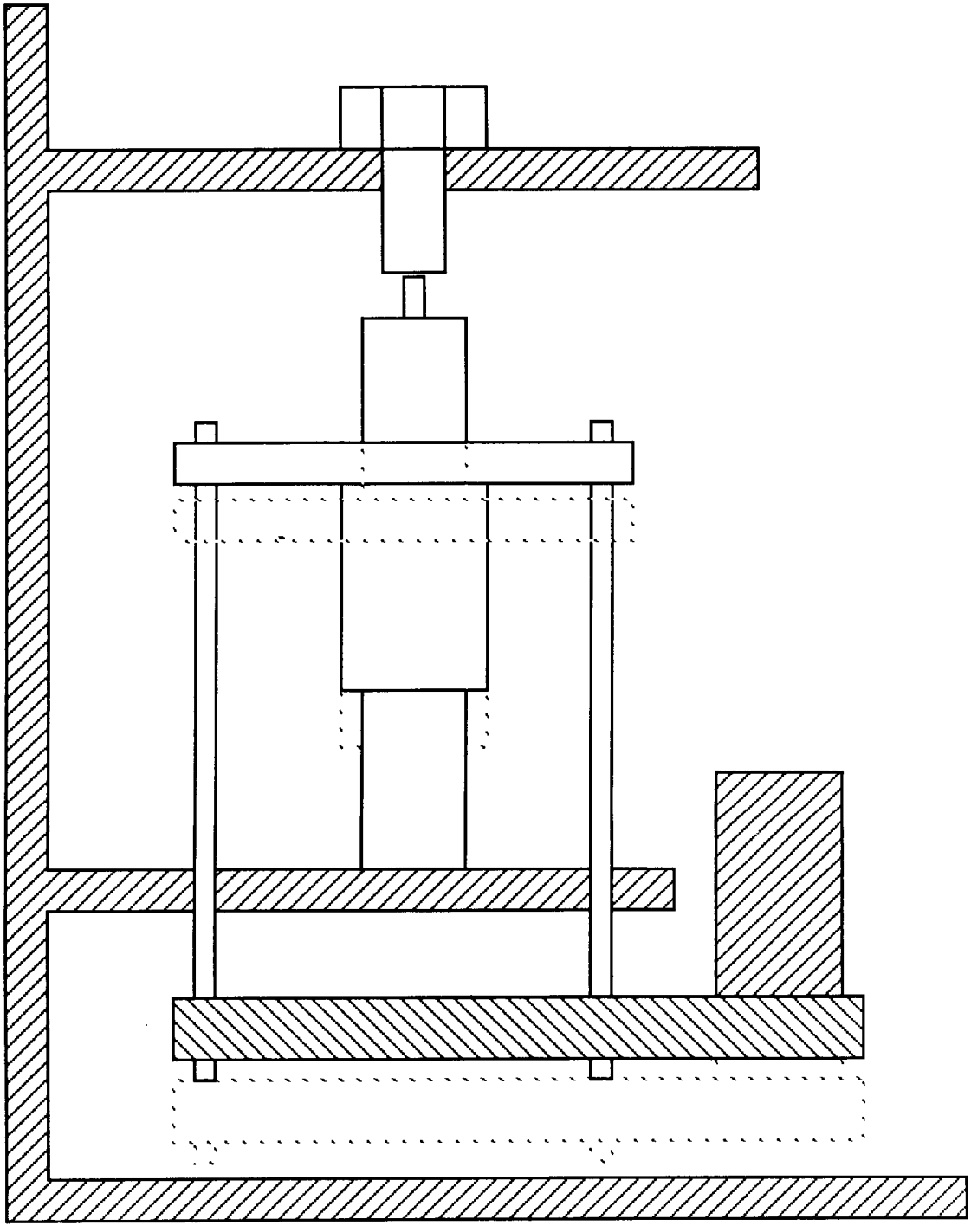

FIGURE 5 PRIMARY IN COMPRESSION BUT EXTENDING, SECONDARY IN COMPRESSION AND COMPRESSING

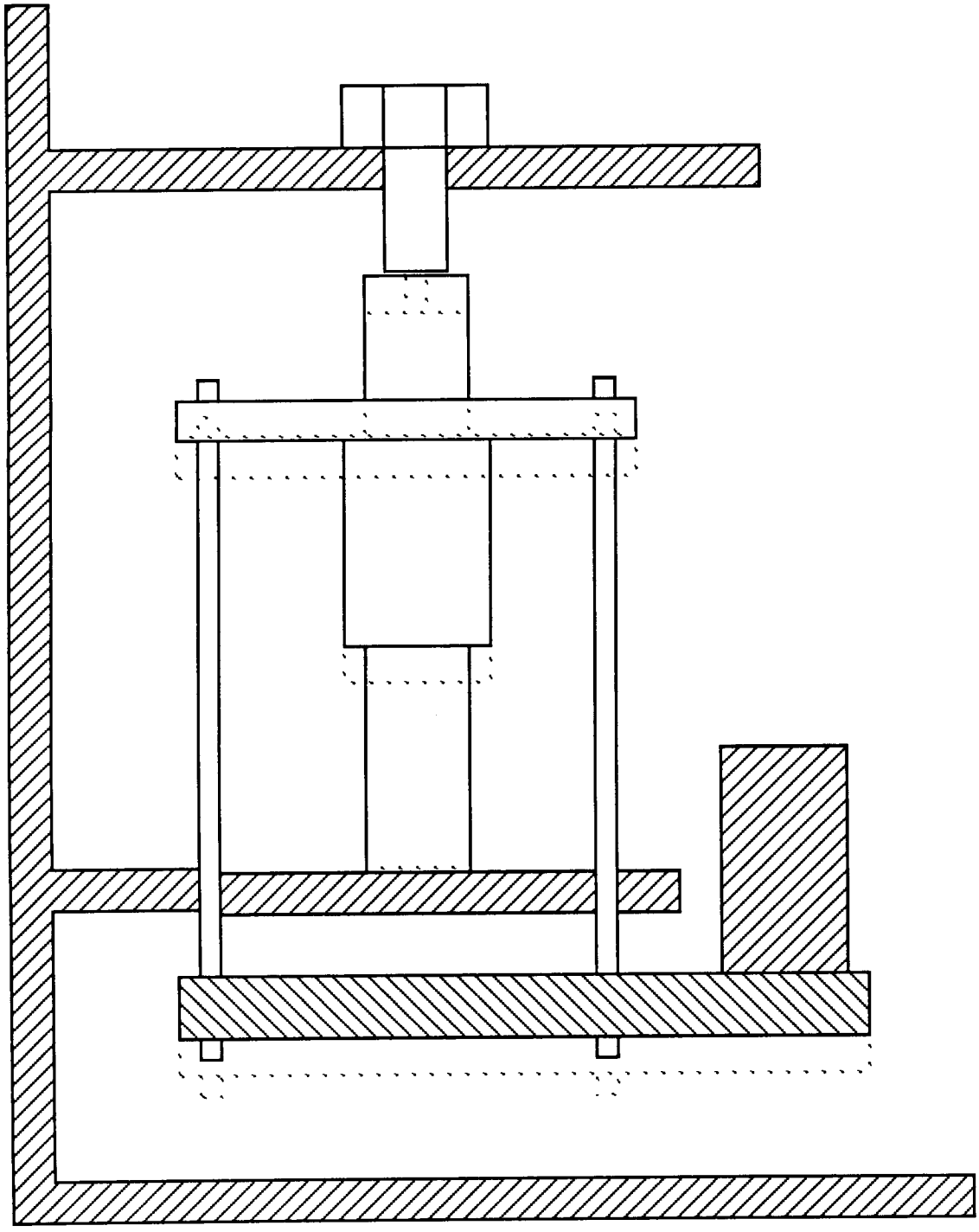

FIGURE 6 PRIMARY IN COMPRESSION AND COMPRESSING, SECONDARY IN COMPRESSION BUT EXTENDING

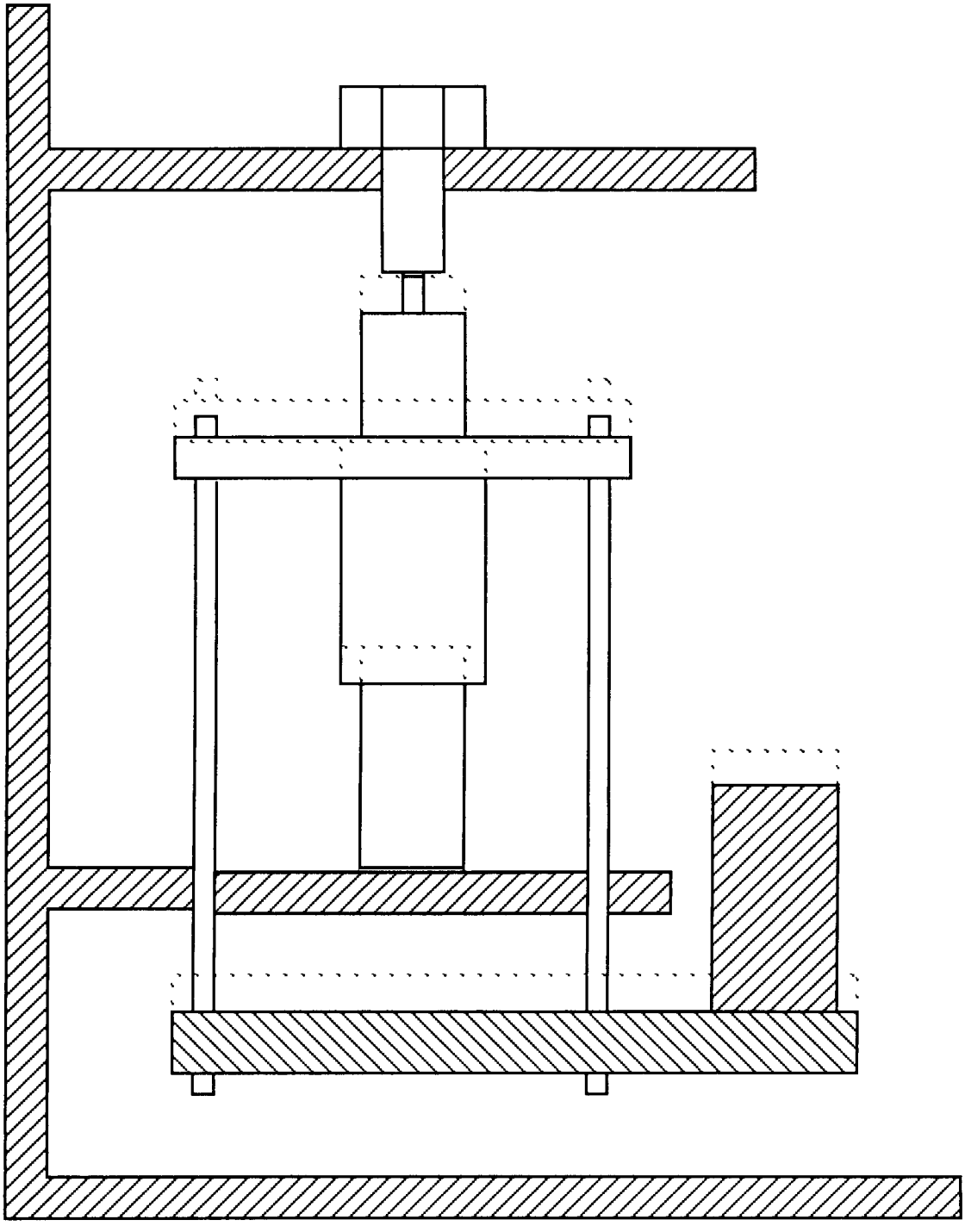

spring piston. Its geometric location is identical to grid point one. Grid point two is located on the plate that bolts the two springs together. Grid point three is located at the intersection of the primary spring and the MK-14 Canister. The base plate adapter is represented by grid point four.

The grid and element numbering system is shown schematically in Figure 7. The X axis is positive downward, and the origin is located at grid point one. The orientation of the Y-Z axes is immaterial for this model.

The gap element is used to simulate the ability of the secondary spring (at grid point 5) to separate from the MK-14 Canister (at grid point 1). When the gap is closed (which occurs at steady state and conditions 3 and 4), the element acts like a rigid bar and causes the secondary spring to work. During conditions 1 and 2, the gap is open, and the secondary spring is isolated. The gap condition during operation is illustrated in Figures 3 through 6.

The rod element is used to model the linear part of the static spring force. The non-linear part is handled as a non-linear load (see further discussion below). The static spring force is used as a reset mechanism to return the assembly to its original position. As such, it will absorb force when it is being compressed and release the force when it is extending from the compressed position. The stiffness is set equal to the linear part of the spring force for both the primary and secondary springs.

For simplicity, a viscous damper element is used to characterize the coulomb damping resulting from the MK-14 Canister pads contacting the AUR. The correct value was determined using an iterative process of running the model and comparing the results to the experimental data.

The non-linear load applied to the model consists of the non-linear static spring force and the velocity dependent spring damping. The non-linear static spring force consists of a preload and a term that is a function of the spring displacement squared. The damping is a function of the velocity to .7 power.

The preload for both springs is ignored. This could be done since the model was constructed at the steady state assembled condition.

The squared term for the primary spring is input according to the liquid spring drawing specifications. The squared term for the secondary spring is ignored. This is done since the anticipated secondary spring displacement is about one inch and after squaring and scaling the resulting force is negligible.

The primary spring damping acts in compression and extension and removes force from the system in either case. The force was generated as a function of the relative velocity of the end points of the spring in accordance with the liquid spring drawing specifications. It was

FIGURE 7 LIQUID SPRING ASSEMBLY FINITE ELEMENT MODEL

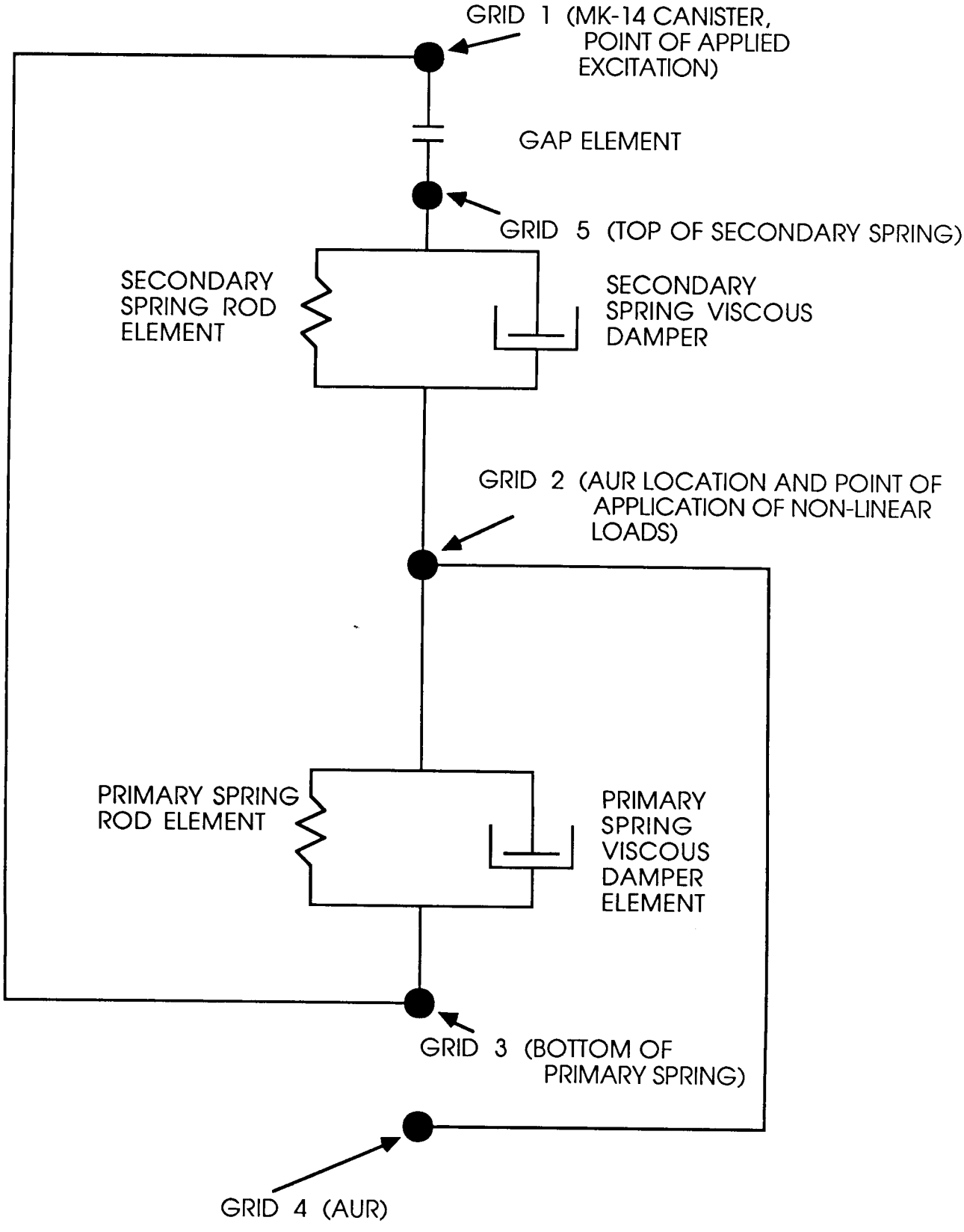

anticipated that a spring failure would result in the loss of extension damping and so the model was constructed to be able to zero this term. The damping of the secondary spring was ignored. This was done since the damping force range specified in the liquid spring drawing is negligible.

The excitation consisted of the MK-14 Canister acceleration. The response in the X or vertical direction was used since it was the primary load direction.

RESPONSE TO NOSC MIL-S-901 MEDIUM-WEIGHT MACHINE SHOCK TESTS

Tests 75 through 86 corresponding to the second canister Launch Test Inert Vehicle (LTIV) series [2] were chosen to validate the finite element model. Selected displacement results are shown in Figures 8 and 9. Model parameters indicate a degradation of the primary compression damping occurring over tests 75 and 76 (see Table 1) with zero effective primary extension damping. This is an indication that the springs were malfunctioning. The post test inspection revealed that three of the four springs had sustained a tension failure at the attachment of the piston rod to the damper plate.

The presence of the compression damping can be explained when one considers how the springs operate as detailed in the preceding section. At the initial pulse the primary spring is compressed, hence the compression damping. As the spring starts to expand, the damper plate (which has broken off from the piston rod, see Figure 2) will be suspended in the fluid as the piston moves away resulting in zero extensional damping. At the conclusion of the test the damper plate will settle onto the piston rod as gravity and time take effect. This provides compression damping at the start of the next test.

Table 1 Optimized Model Parameters for each Test

test no	extension damping (-)	compression damping (-)	initial gap (in)	primary viscous damping (lb/in-sec)	secondary viscous damping (lb/in-sec)
75	5	-2200	0.02	200	50
76	5	-1800	-0.02	100	80
77	5	-1800	-1.1	100	400
78	5	-1800	-0.9	200	200
79	5	-1800	-0.3	200	200
80	5	-1800	-1.6	400	400
81	5	-1800	-1.0	150	50
82	5	-1700	-2.2	20	10
83	5	-1700	-0.5	200	400
84	5	-1700	-1.0	10	50
85	5	-1700	-1.0	10	50
86	5	-1700	-0.5	150	10

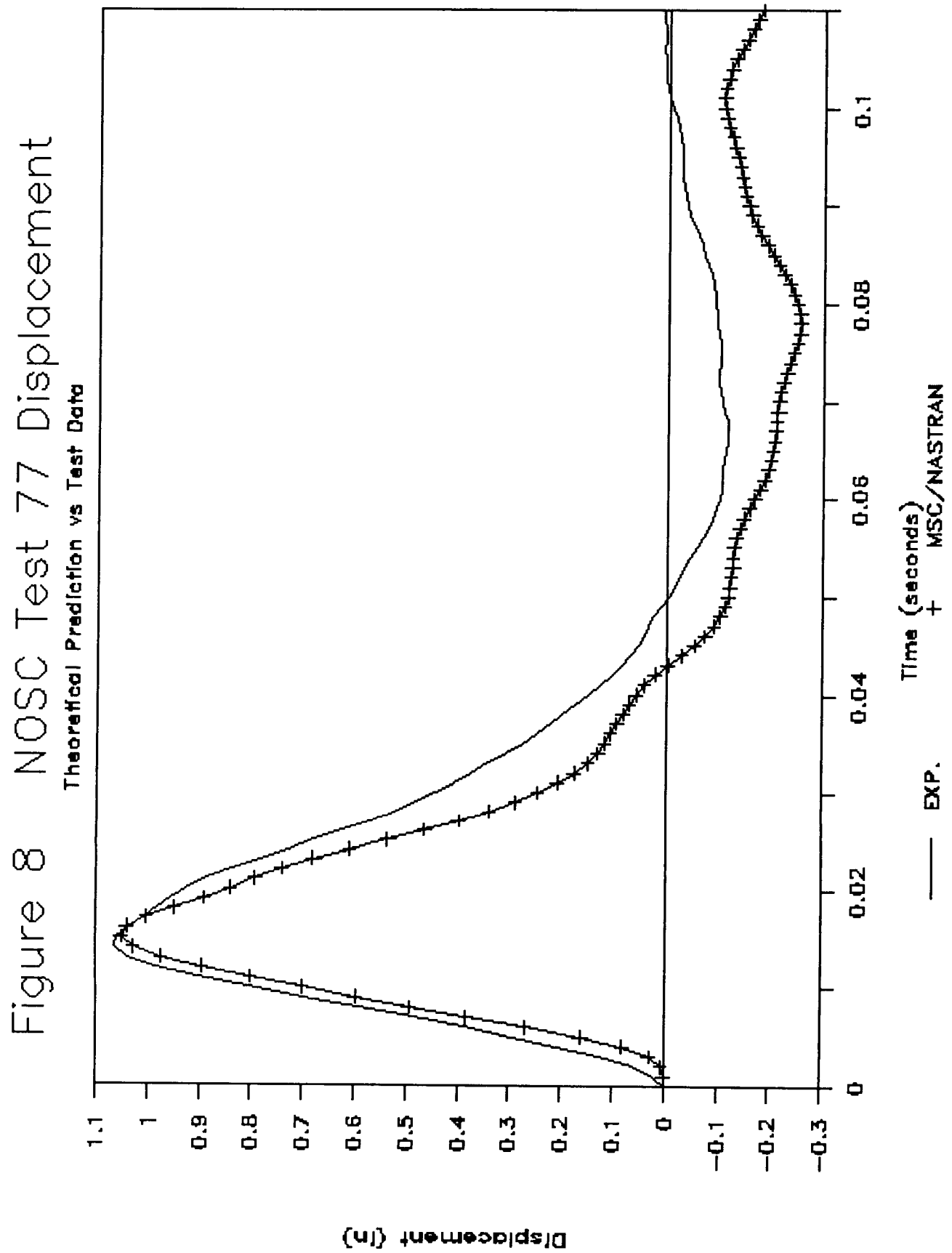
Figure 8 NOSC Test 77 Displacement
Theoretical Prediction vs Test Data
Displacement (in)
1.1
1
0.9
0.8
0.7
0.6
0.5
0.4
0.3
0.2
0.1
0
-0.1
-0.2
-0.3
0
0.02
0.04
0.06
0.08
0.1
Time (seconds)
EXP.
MSC/NASTRAN

Figure 9 NOSC Test 81 Displacement

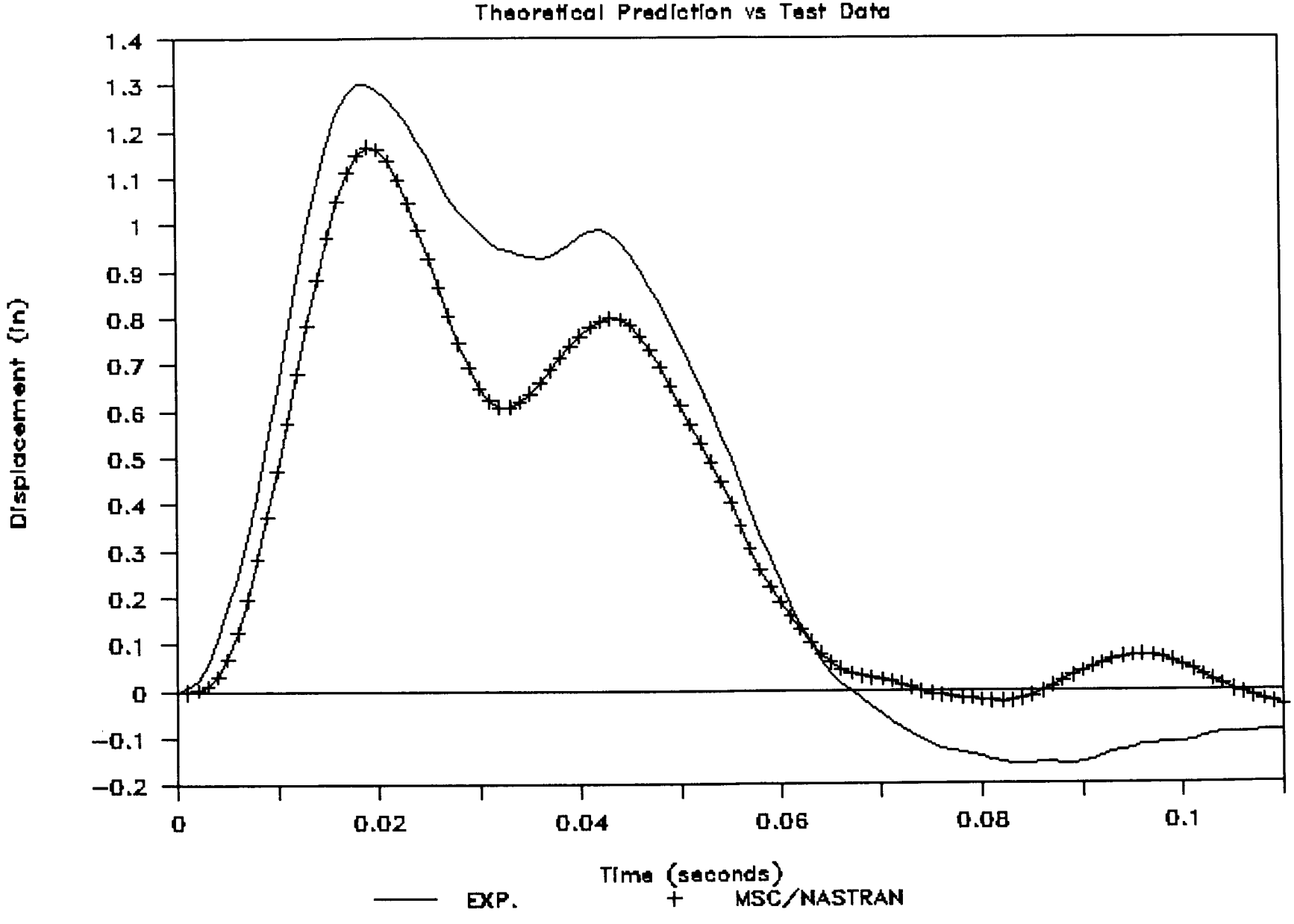

Test 77 (Figure 8) provides an ideal response in that it is relatively easy to divide the MSC/NASTRAN generated curve into the four conditions described previously. Condition one occurs between time zero and fifteen msec and peaks at 1.05 inches. This is a primary spring displacement (the secondary having gapped and so isolated itself at this time) and results in a stored force of 6000 lbs for four springs. The velocity at this time is 0.518 fps which translates into 6500 lbs of force reduced by the springs. Additional force is removed by the friction pads.

Condition 2 occurs between 15 and 42 msec. At 42 msec the 6000 lb spring force has been returned to the MK-14 Canister and the secondary spring gap has closed. No additional force has been removed from the system by the springs. All damping is due to the friction pads.

Condition 3 occurs between 42 and 78 msec. The 0.25 in. peak displacement at this time is an extension of the primary spring and an equal compression of the secondary spring. The deviation from the experimental data during this and the next condition is due to the modeling of the friction pads (coulomb damping) as a viscous damper element. At low velocities, the viscous damper removes less energy while the friction pads ,in reality, are removing more energy due to higher forces.

Condition 4 starts at 78 msec and continues until the displacement returns to zero. This analysis was stopped at 120 msec when most of the energy from the shock had been dissipated. This condition corresponds to a resetting of the spring in preparation for the next test. The system does not return to the pretest condition. This can be seen from Table 1 which shows an initial gap corresponding to the system condition at the end of the previous test. This gap is caused by the friction pads.

RESPONSE TO CG-53 SHOCK TRIAL

After NOSC test validation the model was used to predict TOMAHAWK response to the CG-53 shock trial loading. Predictions and validation were done for TOMAHAWK test missiles designated IOM-A (Inert Operational Missile), IOM-B, IOM-C, LTIV-1, AND LTIV-3.
After the first shot, the procedure was to validate the model using the previous shot data (MK-14 Canister and AUR baseplate accelerations and relative displacement across the liquid springs), scale up this data by a ratio obtained from analysis of the YORKTOWN shock test series to make a prediction for the next shot and, at the conclusion of the next shot, compare predictions with actual data. The YORKTOWN test series was analyzed due to the ship's similar specifications and identical shock geometry to the MOBILE BAY's. The procedure was performed for shots 2 through 4.

Figures 10 through 13 compare the model predictions and subsequent validations with test data. These results are representative of the results for all TOMAHAWK test vehicles. The

FIGURE 10 CG53 SH#4 IOM B

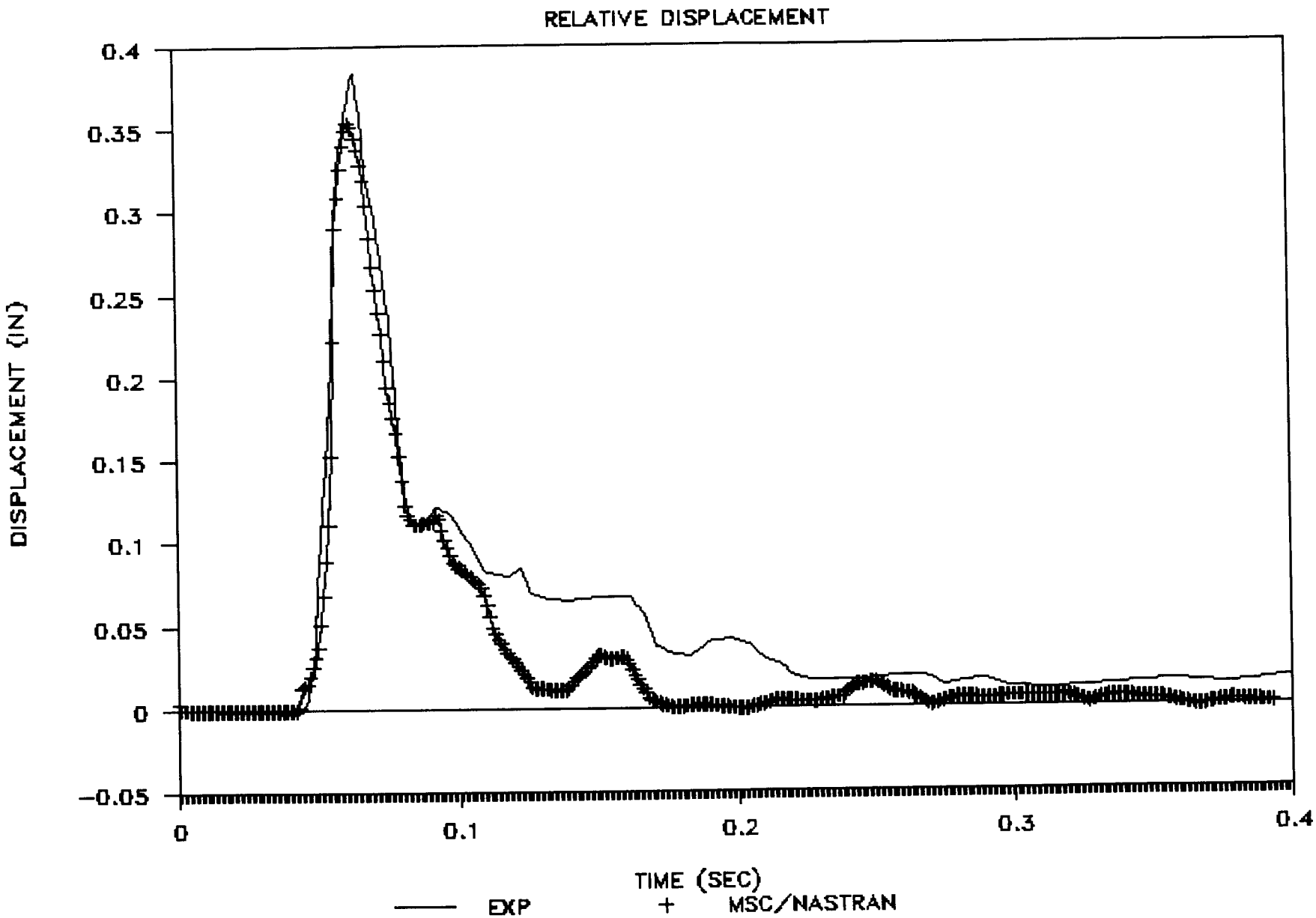

FIGURE 11 CG-53 SH#4 IOM-B

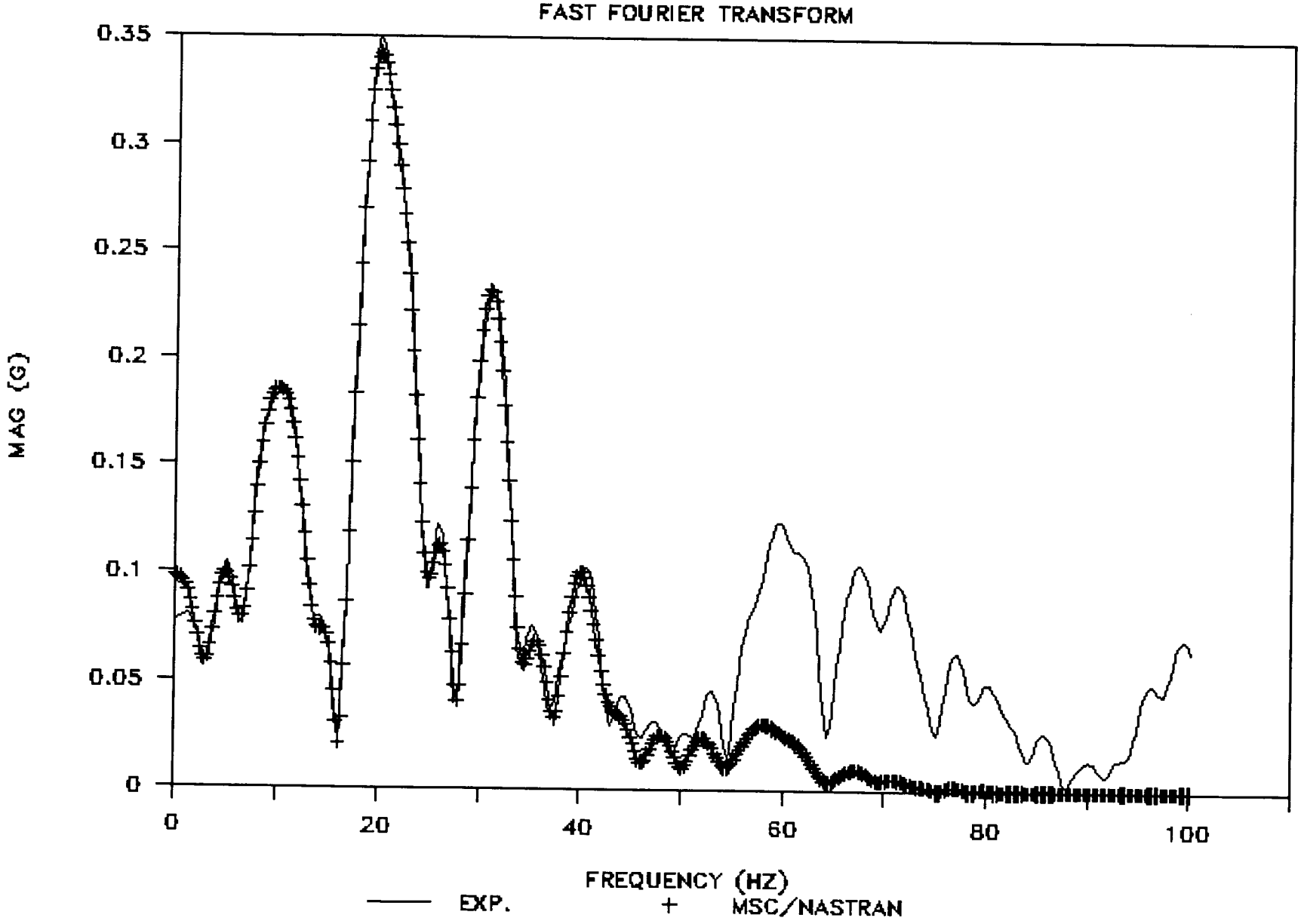

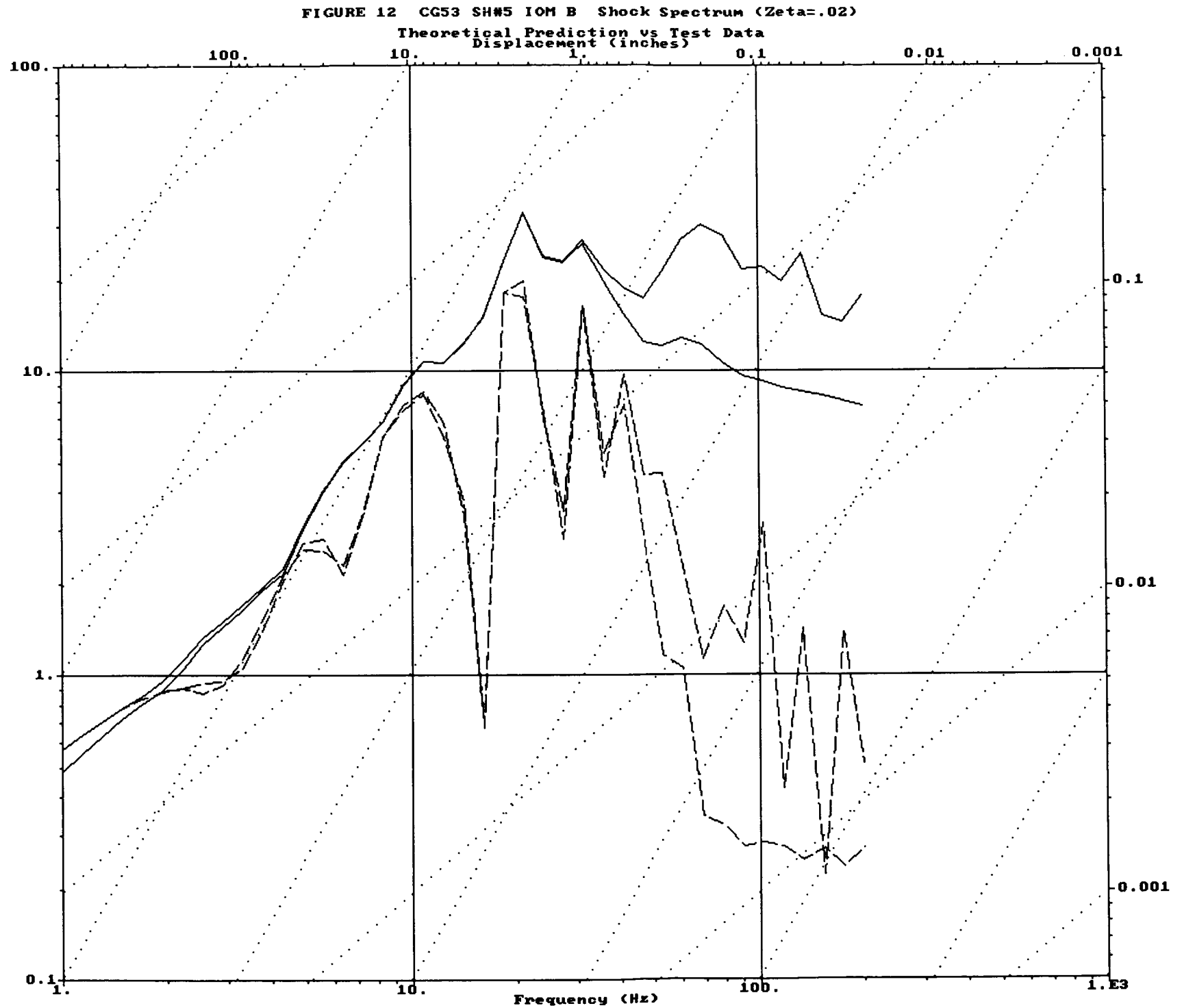
FIGURE 12 CG53 SH#5 IOM B Shock Spectrum (Zeta=.02)
Theoretical Prediction vs Test Data
Displacement (inches)
100.
10.
1.
0.1
0.01
0.001
100.
10.
1.
0.1
Max Accel (g's)
Velocity (ft/sec)
0.1
0.01
0.001
1.
10.
100.
1.E3
Frequency (Hz)

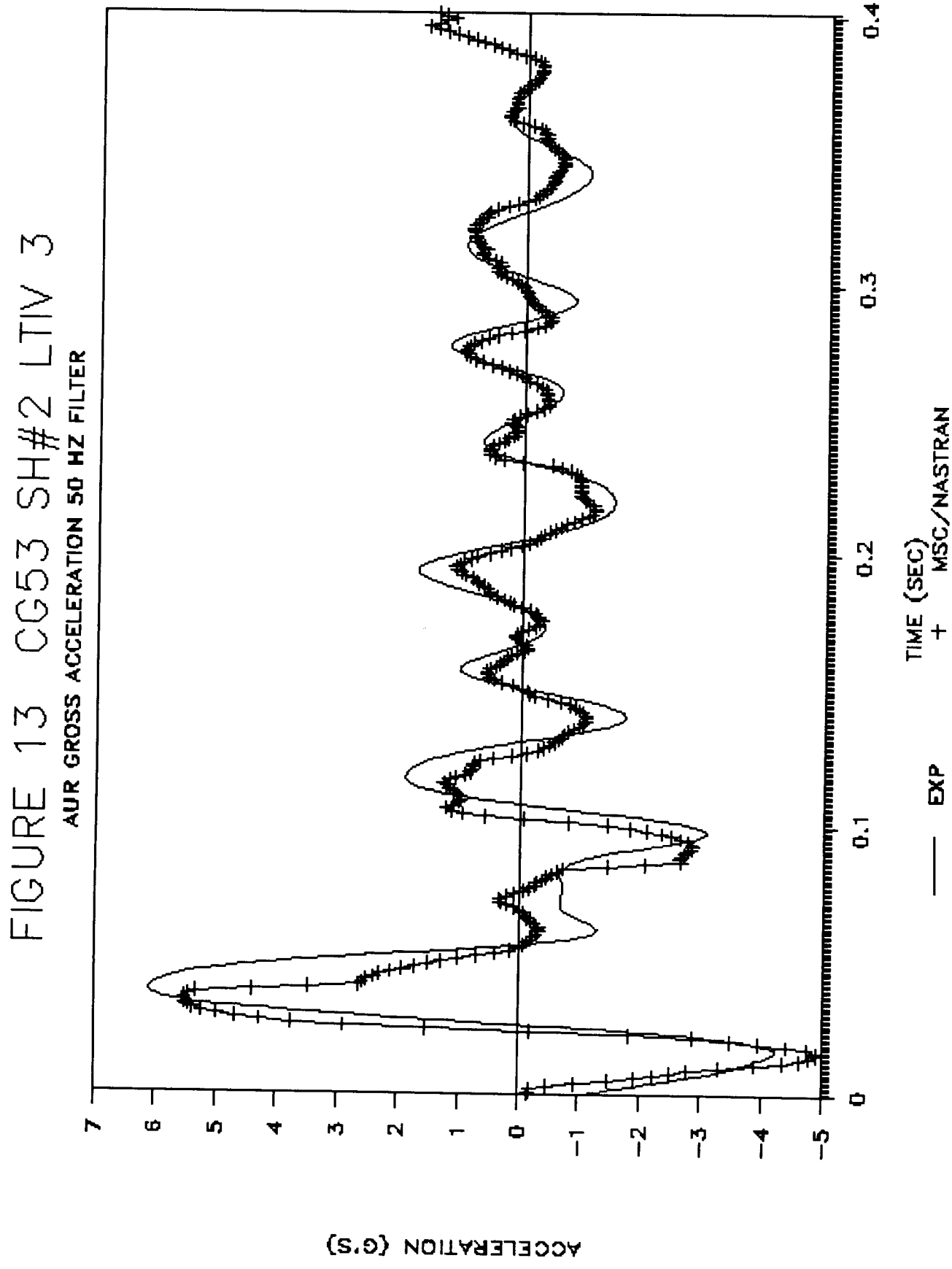
FIGURE 13 CG53 SH#2 LTIV 3
AUR GROSS ACCELERATION 50 HZ FILTER
ACCELERATION (G'S)
7
6
5
4
3
2
1
0
-1
-2
-3
-4
-5
0
0.1
0.2
0.3
0.4
TIME (SEC)
EXP
+ MSC/NASTRAN

model parameters indicated that the springs provided adequate shock isolation with only a slight degradation of primary spring extensional damping.

Figure 10 is a plot of model verification for shot 4 IOM-B relative displacement. Note that conditions 3 and 4 are not as pronounced as in the NOSC tests. This is due to the availability of extensional damping (since the spring is not broken) on the primary spring. Conditions 3 and 4 can be considered as occurring after 100 msec when the system is settling down after its response to the shock.

Figure 11 is a plot of the fast fourier transform of the gross acceleration (experimental and model prediction) for shot 2 LTIV-3 model verification. Figure 12 is a plot of the shock spectrum of the gross acceleration (experimental and model prediction) for shot 4 IOM-B model verification. These figures demonstrate that the majority of energy is concentrated below 50 Hz and the model response is valid to 50 Hz. Therefore, the experimental data is low-pass-filtered at 50 Hz. and compared to the model response (Figure 13) for verification. Based on Figures 10 thru 13 it is concluded that the finite element model accurately represents the physical system.

Figure 14 compares the prediction made for shot 4 with the actual shot results for LTIV-1 relative displacement. This model was first verified for shot 3 before being used for the shot 4 prediction. This comparison indicates that the scaling ratio obtained from analysis of the YORKTOWN test series is reasonable.

Displacement and acceleration predictions agree well with experimental results indicating that the model can successfully track the actual TOMAHAWK performance and that the response from shot to shot is a linear function of the previous shot.

CONCLUSIONS

Successful analysis of non-linear systems is a three step process. First the non-linearities must be identified and quantized. Step two is the selection of an analysis technique and/or computer code that addresses the identified non-linearities. The final step is the validation of the model using system data and the subsequent use of the model in prediction and validation of test results. This technique was illustrated using the TOMAHAWK shock isolation system and MSC/NASTRAN finite element computer code with excellent agreement between model and test results.

REFERENCES

1. MSC/NASTRAN USER'S MANUAL version 65, November 1985.
2. QUICK LOOK REPORT, VLS CANISTER/MISSILE CONFIDENCE SHOCK TEST, TEST 75-86, NOSC, August 1986.

FIGURE 14 CG53 SH#4 LTIV 1 REL. DISPL.